Physics of Plasmas

A perturbative approach to a nonlinear advection-diffusion equation of particle transport

Cite as: Phys. Plasmas **27**, 082901 (2020); https://doi.org/10.1063/5.0003582
Submitted: 03 February 2020 . Accepted: 02 July 2020 . Published Online: 03 August 2020

Dominik Walter, Horst Fichtner, and Yuri Litvinenko

Physics of Plasmas ARTICLE scitation.org/journal/php

A perturbative approach to a nonlinear advection-diffusion equation of particle transport

Cite as: Phys. Plasmas **27**, 082901 (2020); doi: 10.1063/5.0003582
Submitted: 3 February 2020 · Accepted: 2 July 2020 ·
Published Online: 3 August 2020

Dominik Walter,[1,a)] Horst Fichtner,[1] and Yuri Litvinenko[2]

AFFILIATIONS

[1]Institut für Theoretische Physik IV, Ruhr-Universität Bochum, Universitätsstrasse 150, 44780 Bochum, Germany
[2]Department of Mathematics, University of Waikato, P. B. 3105, Hamilton 3240, New Zealand

[a)]Author to whom correspondence should be addressed: dw@tp4.rub.de

ABSTRACT

We explore analytical techniques for modeling the nonlinear cosmic ray transport in various astrophysical environments which is of significant current research interest. While nonlinearity is most often described by coupled equations for the dynamics of the thermal plasma and the cosmic ray transport or for the transport of the plasma waves and the cosmic rays, we study the case of a single but nonlinear advection-diffusion equation. The latter can be approximately solved analytically or semi-analytically, with the advantage that these solutions are easy to use and, thus, can facilitate a quantitative comparison to data. In the present study, we extend our previous work in a twofold manner. First, instead of employing an integral method to the case of pure nonlinear diffusion, we apply an expansion technique to the advection-diffusion equation. We use the technique systematically to analyze the effect of nonlinear diffusion for the cases of constant and spatially varying advection combined with time-varying source functions. Second, we extend the study from the one-dimensional, Cartesian geometry to the radially symmetric case, which allows us to treat more accurately the nonlinear diffusion problems on larger scales away from the source.

I. INTRODUCTION

In recent years, several authors have addressed the nonlinearity of the cosmic ray transport in various astrophysical environments. The latter comprise the interstellar medium (e.g., Ptuskin *et al.*, 2008; Amato and Blasi, 2018; Holcomb and Spitkovsky, 2019), supernova remnants (e.g., Ptuskin, Zirakashvili, and Seo, 2013; Bykov *et al.*, 2014; Perri *et al.*, 2016; Diesing and Caprioli, 2019; Nava *et al.*, 2019), heliospheric shock acceleration (e.g., Lee *et al.*, 2012), and modulation (e.g., Moloto *et al.*, 2018; Shalchi, 2018).

The nonlinearity is most often described by coupled equations for the dynamics of the thermal plasma and the cosmic ray transport (e.g., Wiener *et al.*, 2019) or for the transport of the plasma waves and the cosmic rays (e.g., Nava *et al.*, 2016). Since these models require numerical solution procedures, we have recently investigated analytical and semi-analytical treatments on the basis of nonlinear diffusion equations (Litvinenko *et al.*, 2017; Litvinenko *et al.*, 2019) with the motivation to provide a treatment of the problem of nonlinear cosmic ray transport. These alternatives, which are based on a single advection-diffusion equation with a diffusion coefficient depending on the (gradient of the) particle distribution function, not only complement the development of the more detailed numerical models but also may guide as well as help to test the latter. While in the work of Litvinenko *et al.* (2017) we have concentrated on the implications of the nonlinearity for the so-called anomalous transport (for a review of applications see dos Santos, 2019) in one-dimensional, Cartesian advective-diffusive systems, in the work of Litvinenko *et al.* (2019), we have extended the modeling to time-varying source functions in the absence of advection. We extend these analyses here to systems with radial symmetry and with time-dependent sources as well as non-vanishing advection, which are often of interest in astrophysics, for instance, for the particle transport in the solar wind. The method applied in this paper will be able to deal with advection, as well as time dependent sources, and, therefore, combines the strengths of our previous works, without having the restriction of earlier approaches. To show that the mathematical method we apply in this paper has a general value, we discuss a few additional models in the Appendix.

II. THE NONLINEAR DIFFUSION EQUATION

The diffusive part of the nonlinear transport equation reads

$$\frac{\partial f}{\partial t} = \nabla[D(f)\nabla f], \tag{1}$$

with the diffusion coefficient $D(f)$ depending on the solution $f = f(\vec{r}, t)$. As argued in the work of Litvinenko *et al.* (2017), a reasonable choice for this dependence is in the case of cosmic rays interacting with plasma fluctuations

$$D(f) = D_0(\hat{f}_0/r_0)^{\nu}|\nabla f|^{-\nu}, \nu \geq 0 \tag{2}$$

because it has been shown that $\nu = 1/2$ corresponds to wave energy transfer to the thermal ions interacting with moving magnetic mirrors formed by waves (Zirakashvili, 2000) and $\nu = 2/3$ corresponds to energy dissipation by a Kolmogorov-type energy cascade (Ptuskin and Zirakashvili, 2003). The normalization constants $\hat{f}_0$ and r_0 represent a normalization in their respective units to give D the correct dimensions for a diffusion coefficient. $D(f)$ is an effective diffusion coefficient, where $\hat{f}_0$ and r_0 were introduced such that the constant D_0 is always the reference diffusion coefficient for the case $\nu = 0$, i.e., linear diffusion.

The corresponding nonlinear operator $\Delta_p f = \mathrm{div}(|\nabla f|^{p-2}\nabla f)$ is also known as p-Laplacian and has been studied in mathematics and applied science, e.g., in the context of porous media and rheology. While the resulting form of diffusion has been named n-diffusion (Philip, 1961), the corresponding equations are called p-Laplace equation (Vázquez, 2017) or p-Poisson equation (Hartmann and Weimar, 2018).

In the work of Litvinenko *et al.* (2017), we have made first steps to describe the behavior of particle distributions under the influence of this kind of nonlinear diffusion. On the one hand, we used self-similar analytical solutions, as, for example, reviewed by Dresner (1983), to describe, e.g., diffusive escape from extended reservoirs in a one-dimensional, Cartesian geometry. On the other hand, we have complemented these analytical considerations with numerical simulations to investigate the influence of an additional advection of the background plasma on the particle distribution function. While this first study was limited to source functions being constant with respect to time, in the work of Litvinenko *et al.* (2019), we have extended this analysis, for the case of pure diffusion, to time-variable sources.

We expand our previous work in a twofold manner. First, instead of employing an integral method, as in Litvinenko *et al.*, (2019) to the case of pure nonlinear diffusion, we apply an expansion technique to the advection-diffusion equation to derive linear equations that are semi-analytically solvable with fundamental solutions. This allows an improved systematic analysis of the effect of nonlinear diffusion for the cases of constant as well as spatially varying advection, both with time-varying source functions. Second, we extend the study from the one-dimensional, Cartesian geometry to the radially symmetric case. This allows us to treat the nonlinear diffusion problems on larger scales away from the source because various astrophysical systems can, to a good approximation, be treated as spherically symmetric. Consequently, after a thorough study of various Cartesian cases in Sec. III, we extend the investigation to the radial geometry in Sec. IV. We summarize the findings and draw conclusions in Sec. V.

III. SEMI-ANALYTICAL APPROACH TO NONLINEAR ADVECTION-DIFFUSION EQUATIONS IN A ONE-DIMENSIONAL CARTESIAN GEOMETRY

A. Basic theory

Let us consider a linear partial differential equation with a linear operator $\mathcal{L}$ acting on a function f

$$\mathcal{L}f = S, \tag{3}$$

with an inhomogeneity S. To find solutions for f, it is sufficient to determine the fundamental solution Γ, which solves $\mathcal{L}\Gamma = \delta_0$, where δ_0 is a delta function of all variables of the operator $\mathcal{L}$. Through the convolution of $\Gamma * S$, one derives a solution to (3).

Since the problem of this paper, however, is a nonlinear one, one cannot apply this exact method directly. We seek solutions of the nonlinear diffusion-advection equation, which reads in one spatial dimension x

$$\frac{\partial f}{\partial t} + V\frac{\partial f}{\partial x} = \frac{\partial}{\partial x}\left(D(f)\frac{\partial f}{\partial x}\right) + \frac{1}{3}\frac{dV}{dx}\frac{\partial f}{\partial s} + S. \tag{4}$$

Here $V = V(x)$ is an advection speed, $S = S(x, s, t)$ is a source, $s = \ln(p/p_0)$ is the logarithm of particle momentum normalized to a reference momentum p_0, and $D(f)$ is of the form given in Eq. (2). We assume that the transport equation is fully normalized and the parameters discussed above are the normalized representations. This nonlinear equation can be solved approximately by expanding f in a series with respect to the nonlinearity parameter ν

$$f = f_0 + \nu f_1 + \nu^2 f_2 + \cdots. \tag{5}$$

The idea of expanding nonlinear equations with respect to a nonlinearity parameter has been studied before, see, for example, Bender *et al.* (1989) and Bender *et al.* (1991), or as an even earlier example Kath and Cohen (1982). Bender *et al.* (1991) applied this method to the Burgers- and the Korteweg-De Vries equation, while Kath and Cohen (1982) studied a nonlinear diffusion model. Inserting the expansion into Eq. (4) and equating the orders of ν, one receives a set of equations to solve. First note that expanding the linear parts of Eq. (4) is straightforward, so the only term of interest is the diffusion part. It follows

$$\frac{\partial}{\partial x}\left(D(f)\frac{\partial f}{\partial x}\right) = \frac{\partial}{\partial x}\left(\left|\frac{\partial f}{\partial x}\right|^{-\nu}\frac{\partial f}{\partial x}\right) = (1-\nu)\left|\frac{\partial f}{\partial x}\right|^{-\nu}\frac{\partial^2 f}{\partial x^2} = (1-\nu)|f_x|^{-\nu}f_{xx}. \tag{6}$$

In the last step, we introduced the short notation $\frac{\partial f}{\partial x} = f_x$ and $\frac{\partial^2 f}{\partial x^2} = f_{xx}$, etc., which we will continue to use from now on. Furthermore,

$$|f_x|^{-\nu} = \exp[-\nu\ln|f_x|] \approx 1 - \nu\ln|f_x| + \frac{1}{2}\nu^2\ln^2|f_x|. \tag{7}$$

After inserting Eq. (5) in this last equation, one can give an approximation for $\ln|f_x|$ via Taylor development,

$$\ln|f_x| = \ln|f_{0,x} + \nu f_{1,x} + \nu^2 f_{2,x}| \approx \ln|f_{0,x}| + \nu\frac{f_{1,x}}{f_{0,x}} + \frac{\nu^2}{2}\left(\frac{2f_{2,x}}{f_{0,x}} - \frac{f_{1,x}^2}{f_{0,x}^2}\right) + \cdots. \tag{8}$$

Using this in Eq. (7), one derives the following expression for the diffusion term in Eq. (4):

$$(1-\nu)|f_x|^{-\nu}f_{xx} \approx (1-\nu)\left(1 - \nu\left[\ln|f_{0,x}| + \nu\frac{f_{1,x}}{f_{0,x}}\right] + \frac{\nu^2}{2}\ln^2|f_{0,x}| + \cdots\right) \times \cdot\left(f_{0,xx} + \nu f_{1,xx} + \nu^2 f_{2,xx} + \cdots\right). \tag{9}$$

After inserting all those expressions into Eq. (4), it gives the following set of equations:

$$\mathcal{L}_{\rm cart} f_0 = S = Q_0, \tag{10}$$

$$\mathcal{L}_{\rm cart} f_1 = -D_0\big(1+\ln|f_{0,x}|\big) f_{0,xx} = Q_1, \tag{11}$$

$$\mathcal{L}_{\rm cart} f_2 = -D_0\left(\frac{f_{1,x}}{f_{0,x}} - \frac{1}{2}\ln^2\big(|f_{0,x}|\big) - \ln\big(|f_{0,x}|\big)\right) f_{0,xx} - D_0\big(1+\ln\big(|f_{0,x}|\big)\big) f_{1,xx} = Q_2. \tag{12}$$

Here, the operator $\mathcal{L}_{\rm cart}$ is defined as

$$\mathcal{L}_{\rm cart} = \frac{\partial}{\partial t} + V\frac{\partial}{\partial x} - D_0\frac{\partial^2}{\partial x^2} - \frac{1}{3}\frac{dV}{dx}\frac{\partial}{\partial s}. \tag{13}$$

These are linear equations, solvable with fundamental solutions. In the following, three principal cases are studied, namely, constant advection $V = const.$, a spatially varying advection speed $V(x)$, both with a source varying as a power law in time, and pulse-like sources $S(t)$.

B. Case 1: Constant advection

With $V \neq V(x)$, the terms containing the derivatives of f with respect to to s in Eqs.(4), (10), (11), and (12) vanish. According to the theorem by Malgrange–Ehrenpreis (e.g., Yosida, 1980), there exists a fundamental solution for the resulting simplified form of Eq. (10) with $S(x,t) = \delta(x)\delta(t)$. This solution can be found by a Fourier transform with respect to the space coordinate x, which yields

$$\frac{\partial g}{\partial t} + 2\pi i k V g + 4\pi^2 k^2 D_0 g = \delta(t), \tag{14}$$

with k denoting the wavenumber and g the Fourier transform of f. This equation can be solved straightforwardly using the variation of parameters, and the solution takes the form

$$g = \exp\big(-4\pi^2 D_0 k^2 t - 2\pi i k V t\big). \tag{15}$$

The inverse Fourier transform gives the fundamental solution Γ

$$\Gamma = \frac{1}{\sqrt{4\pi D_0 t}}\exp\left(-\frac{(x-Vt)^2}{4D_0 t}\right), \tag{16}$$

with which a solution of the differential equations for f expanded in ν can be derived by convoluting Γ with the right-hand side of the equation for f_i.

In this paper, we consider source terms of the form $S(x,s,t) = S_0 t^\alpha \delta(x)$ or combinations thereof, representing a particle injection at $x = 0$ with a (combination of) power law(s) in time ($\alpha = 0$ refers to a constant source and represents the case that was discussed in Litvinenko *et al.*, 2017). For such sources, the solution for the zeroth order can be obtained by an integral over time. While it cannot be evaluated analytically, it can be solved straightforwardly numerically.

Corresponding results are presented in Fig. 1, where this semi-analytic solution was tested for low values of ν up to the second order of approximation and a time power law with $\alpha = 2$. The reference case $\nu = 0$, i.e., that of linear diffusion, shows the solution at time $t = 1$ and has the expected structure: a peak at the source location $x = 0$ and an asymmetry due to the nonvanishing advection speed. In this case, the zeroth-order approximation is identical with the exact solution. Because for the numerical code the delta function has to be approximated via an exponential, i.e., $\delta(x) \approx (\pi a)^{-1/2}\exp(-x^2/a^2)$, where a is a small constant, it can actually not reproduce the exact solution, which is obtained when analytically using the exact delta function for the zeroth order (red dashed line). This is verified by using the above exponential in the zeroth-order approximation (green dashed line), which is then identical with the numerical solution (solid line). The use of the latter appears justified if we use a sufficiently narrow source, i.e., a sufficiently small.

The other three panels illustrate the first and second-order approximations resulting from Eqs. (11) and (12) for increasing ν-values, where the corresponding linear case is represented by the zeroth order approximation. The case $\nu = 1/4$ for which the approximation evidently works well reveals the effect of the nonlinear diffusive behavior: there occurs a flattening of the spatial distribution which is indicative of an enhanced spatial diffusion being consistent with a decreased (modulus of the) spatial gradient. The numerical solutions for the two further cases for $\nu = 1/2$ and $\nu = 2/3$ reveal that this flattening leads to a reduced asymmetry of the distribution around the injection location, meaning that the spatial diffusion is gradually dominating the advection, which appears to play a less significant role for $\nu = 2/3$. Also evident from the four panels is the decreasing accuracy of the first and second-order approximation, which is clearly not sufficient for $\nu \gtrsim 0.5$. Furthermore one can see that the second-order approximation does a slightly better job at describing the slopes of the distribution function, even at higher values of ν.

Figure 2 illustrates the behavior of the nonlinear solution for $\nu = 1/2$ in dependence of the source strength, the diffusion coefficient, and the advection speed. The figure reveals that the second-order approximation again does fit the numerical solutions a bit better than the zeroth and first order approximations. Comparing the first and second panels in this figure, one can see that there is a visible change in the precision of the approximation, illustrating that this precision is strongly dependent on the diffusion coefficient. Comparing the second and fourth panels, it can be seen that the precision of the approximation also depends on the chosen velocity, but it does not seem to affect it as much as the diffusion coefficient. The third panel in comparison to the first one shows that the precision of the approximations does not seem to be affected much by the chosen source strength.

Using these results, we can now proceed to extend the transport equation by introducing a spatially varying advection speed and an adiabatic energy change.

C. Case 2: Linear decreasing convection

To make the transport model better suited for astrophysical applications, we wish to include more general forms of $V(x)$. The simplest case would be to assume that $V(x)$ is linear, so we assume that $V(x) = V_0 - bx$, where b is a constant. This model can be justified by the results of, e.g., Isenberg (1986) and Fahr and Fichtner (1992). Furthermore, we will assume a source that is independent of s so that no dependence of the momentum will be shown. This results in a vanishing of the $\frac{1}{3}\frac{dV}{dx}\frac{\partial f}{\partial s}$ term in Eq. (13). We will take a closer look at systems with momentum and energy dependence in future works.

The derivation of the fundamental solution to this problem is very similar to the derivation of the problem with a constant advection speed. After a Fourier transform with respect to x, i.e., $\Gamma(x,t) \to g(k,t)$, the problem takes the form

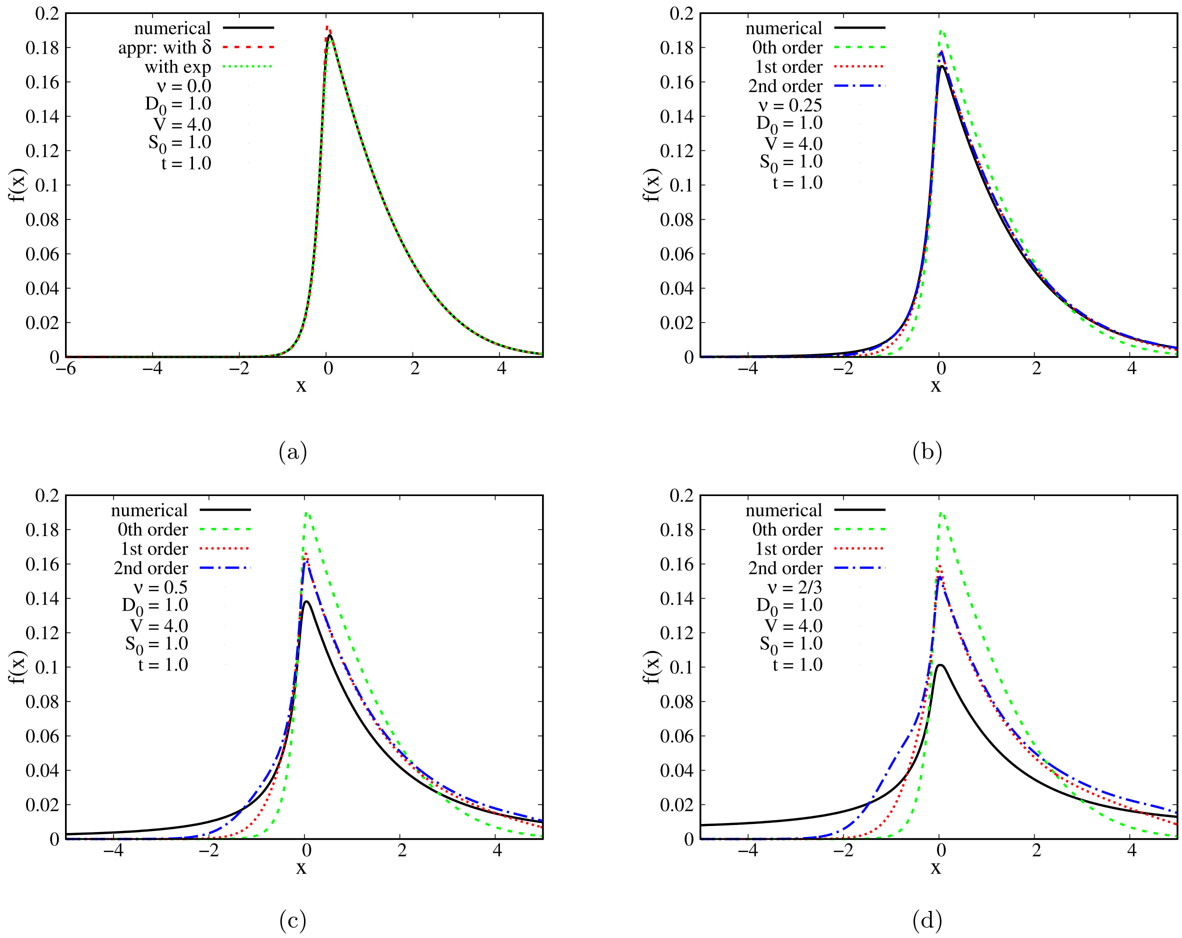

FIG. 1. Solution for a source with a time dependence of $\sim t^\alpha$, with $\alpha = 2$. Comparison of the analytical approximation up to the second order with numerical results. In the four panels, the cases (a) $\nu = 0$, (b) $\nu = \frac{1}{4}$, (c) $\nu = \frac{1}{2}$, and (d) $\nu = \frac{2}{3}$ are shown at $t = 1$. The parameters are $D_0 = 1$, $V = 4$, and $S_0 = 1$.

$$\frac{\partial g}{\partial t} + \left(2\pi i k V_0 + b + 4\pi^2 k^2 D_0\right) g + bk\frac{\partial h}{\partial k} = \delta(t). \tag{17}$$

Introducing a new parameter τ to parameterize the characteristics of the equation, one obtains the equations

$$\begin{aligned} \frac{dt}{d\tau} &= 1 \\ \frac{dk}{d\tau} &= bk \\ \frac{dg(\tau)}{d\tau} + \left(2\pi i k V_0 + b + 4\pi^2 k^2 D_0\right) h(\tau) &= \delta(\tau). \end{aligned} \tag{18}$$

The solution to this set of equations reads as follows:

$$\begin{aligned} t &= \tau \\ k &= k_0 \exp(b\tau) \\ g(\tau) &= \exp\left[-\frac{2\pi i k_0 V_0}{b}(\exp(b\tau) - 1) - b\tau - \frac{2\pi^2 k_0^2 D_0}{b}(\exp(2b\tau) - 1)\right] \end{aligned} \tag{19}$$

or expressed in the old coordinates t and k

$$g(k,t) = \exp\left[-\frac{2\pi i k V_0}{b}\left(1 - \exp(-bt)\right) - bt - \frac{2\pi^2 k^2 D_0}{b}\left(1 - \exp(-2bt)\right)\right]. \tag{20}$$

This equation can be Fourier-back-transformed, and the result is the function Γ we were searching for,

$$\Gamma(x,t) = \frac{\sqrt{b}}{\sqrt{2D_0\pi}\sqrt{1 - \exp(-2bt)}} \cdot \exp\left\{-\frac{\left(V_0(\exp(-bt) - 1) + bx\right)^2}{2D_0 b\left(1 - \exp(-2bt)\right)}\right\} \exp\{-bt\}. \tag{21}$$

As a check of the calculation, we note that in the limit $b \to 0$ this fundamental solution reduces to the well-known fundamental solution of the heat equation.

As before, we can use this fundamental solution to derive specific forms of $f_0, f_1 \ldots$ in Eqs. (10)–(12) (and higher orders, if wanted).

In Fig. 3, three examples are plotted to illustrate the different behaviors of the analytical approximations in comparison to the

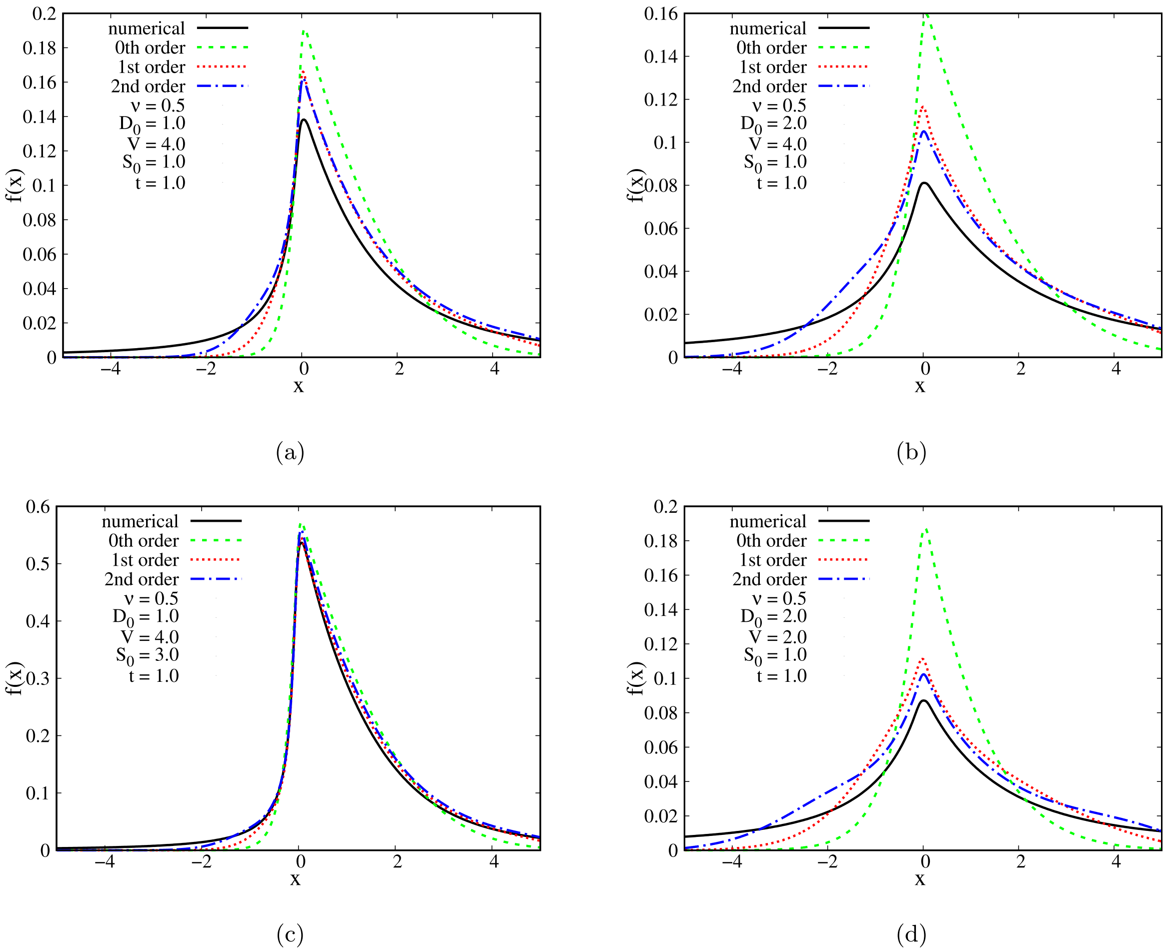

FIG. 2. Solution for a source with a time dependence of $\sim t^\alpha$ with variations of the parameters S_0, D_0, and V with a fixed nonlinearity parameter $\nu = \frac{1}{2}$: (a) $S_0 = 1$, $D_0 = 1$, $V = 4$, (b) $S_0 = 1$, $D_0 = 2$, $V = 4$, (c) $S_0 = 3$, $D_0 = 1$, $V = 4$, and (d) $S_0 = 1$, $D_0 = 2$, $V = 2$ at time $t = 1$ and $\alpha = 2$.

numerical results. The first two panels represent the case $V_0 = 4$ and $b = 0.5$, so it has the same values as the first panel in Fig. 2 at $x = 0$. The next two panels show the results for a changed value of V_0 and the last two panels for a changed $b = 1.5$. As the results show, the quality of the analytical approximation does not change much. The second order approximation does a slightly better job at fitting the numerical curve, specifically in the tails.

Deriving a fundamental solution for a different kind of velocity profile tends to be very difficult, so instead we will now focus on taking a look at a different kind of source.

D. Pulse-like source functions

Another point of physical interest is the behavior of the solutions for different time dependencies. Up to this point, the time dependence of the source term was assumed to be of the form t^α. From a physics point of view, such continuous but non-constant injections are unrealistic. A more acceptable model would contain a pulse-like source, a box function shaped injection, or even a periodic function. Using the derived fundamental solutions above, all such problems are solved by quadrature. If one assumes for the case of constant advection, a time-dependent source of the form $S(x,t) = \delta(x) \cdot (t - \frac{t^2}{t_0})$ for $0 \leq t \leq 1$ and $S = 0$ otherwise. We will again assume that the transport equation is fully normalized and will for simplicity choose to have $t_0 = 1$ in the entire paper. The result for the zeroth order is the difference between the two integrals

$$f_0(x,t) = \int_0^1 t' \Gamma(x, t - t') dt' - \int_0^1 t'^2 \Gamma(x, t - t') dt'. \qquad (22)$$

The higher orders would depend on this zeroth-order solution as they did in Eqs. (11) and (12). The results can again be compared with numerical solutions of the resulting differential equations. The most prominent difference between such time dependence and the simple t^α source is the fact that after a specific time the injection ceases and the solution represents the results of a diffusing distribution that will tend to zero for $t \to \infty$.

To illustrate the solution for a pulse-like source function, we consider the transport Eq. (4) with a constant advection and $S = S_0 \cdot (t - t^2)\delta(x)$ for $0 \leq t \leq 1$ and zero otherwise. The resulting particle distributions were computed for three different sets of parameters D_0, V, and S_0, and for $\nu = \frac{1}{4}$. The computations are presented in Fig. 4,

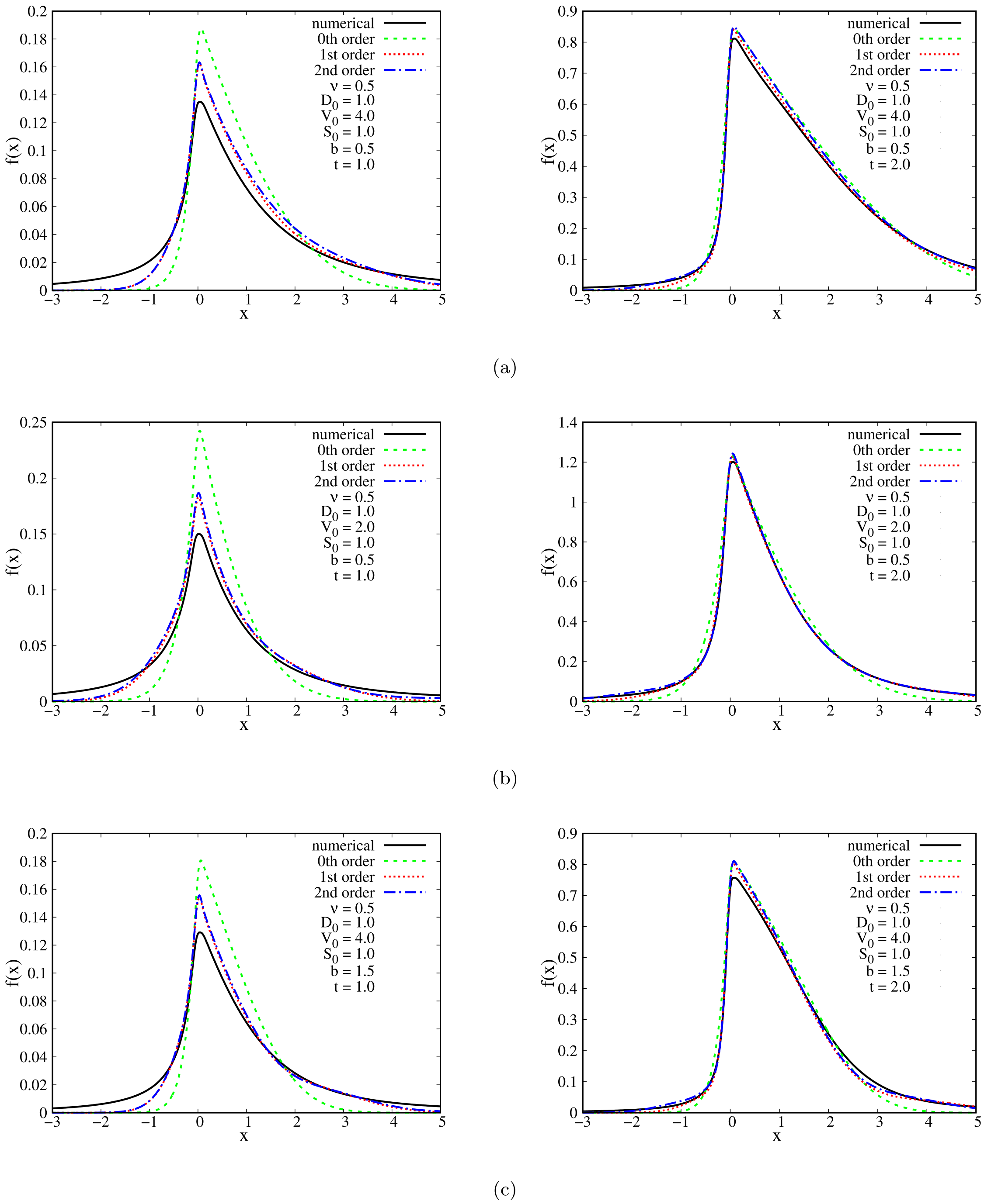

FIG. 3. Solution for variations of the parameters S_0, D_0, and V_0 with a fixed nonlinearity parameter $\nu = \frac{1}{4}$: (a) $S_0 = 1$, $D_0 = 1$, $V_0 = 4$, $b = 0.5$, (b) $S_0 = 1$, $D_0 = 2$, $V_0 = 2$, $b = 0.5$, and (c) $S_0 = 3$, $D_0 = 1$, $V_0 = 4$, $b = 1.5$ and at times $t = 1$ (left) and $t = 2$ (right) and with $\alpha = 2$.

where the left column shows the time evolution of the particle distribution at a point in space downstream of the particle source and the right column shows the evolution at the particle source. The computation was performed assuming a vanishing gradient at $x = 10$ and a vanishing diffusion flux of the form $Vf - D_0|\frac{\partial f}{\partial x}|^{-\nu}\frac{\partial f}{\partial x}$ at $x = -10$, which was the lower boundary. This condition was chosen because in a steady state convection and diffusion have to balance each other in the upstream regime.

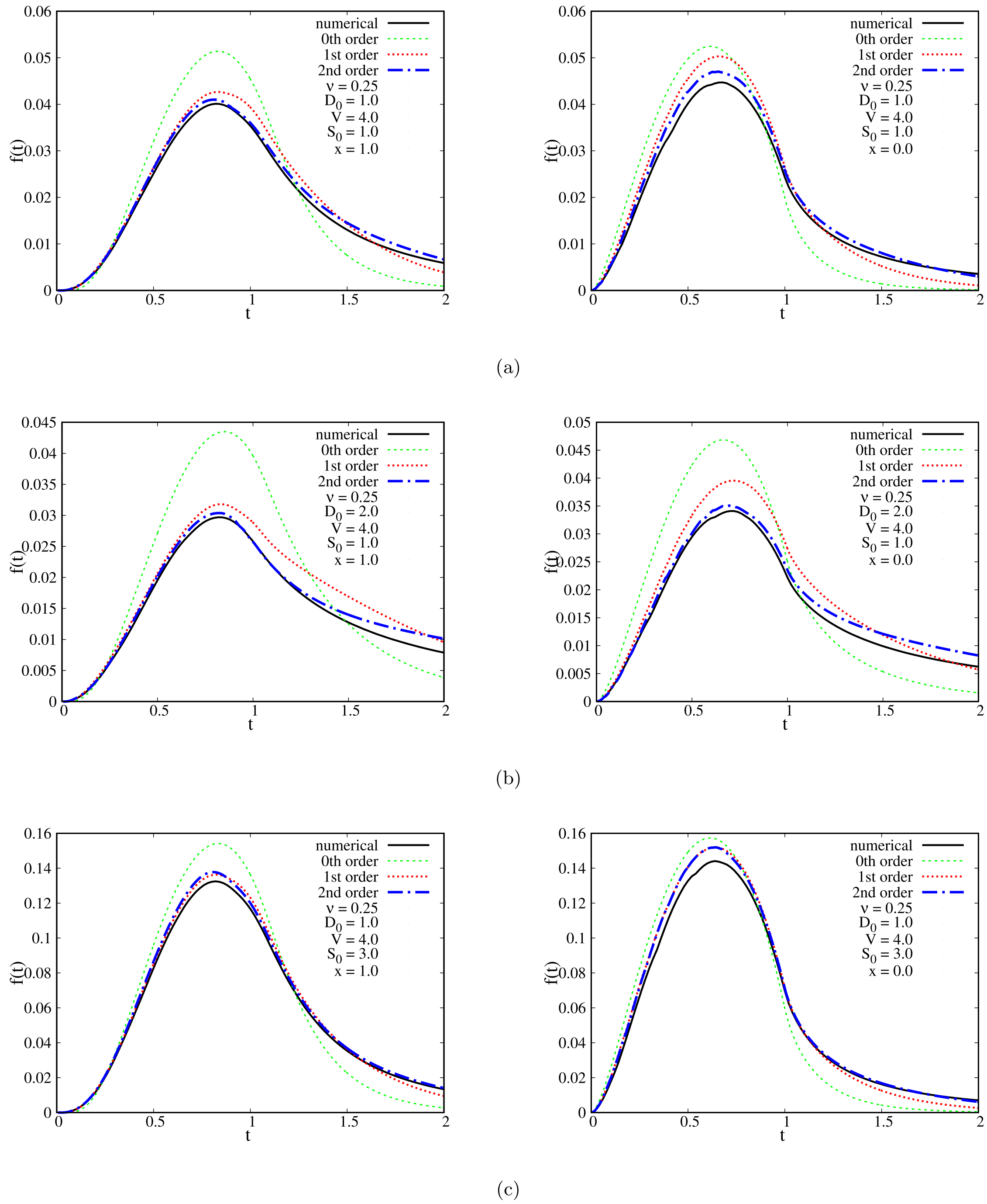

FIG. 4. Solution for a pulse-like particle source and variations of the parameters S_0, D_0, and V with a fixed nonlinearity parameter $\nu = \frac{1}{4}$: (a) $S_0 = 1$, $D_0 = 1$, $V = 4$, (b) $S_0 = 1$, $D_0 = 2$, $V = 4$, and (c) $S_0 = 3$, $D_0 = 1$, $V = 4$, and at distance $x = 1$ (left) and $x = 0$ (right) from the source.

Again the results show that the nonlinear diffusion has a broadening impact: in comparison to the linear case (again represented by the zeroth order approximation), the value of the particle distribution at a fixed point in space (represented by the examples of $x = 0$ and $x = 1$ in the figure) does not reach the same height, while asymptotically the value stays higher. This can be interpreted as particles diffusing away faster in the nonlinear case. On the other hand, particles can stay longer at the fixed points in space we chose for the figure because their diffusion can now resist the advection longer than before. In terms of the quality of the analytical approximations, the same observations as before apply: the first order does well for most cases, with decreasing accuracy for higher diffusion coefficients, and the second-order approximation, generally speaking, does a better job at approximating the slopes of the solution and is an almost exact representation of the numerical solution for early times and late times. If you look at the middle right panel of Fig. 4, it seems like the first order approximation does lie closer to the numerical solution. On the other hand, one can see that the first order approximation has a much steeper slope, so that for later times than pictured in this particular panel again the second order is more precise. In fact, one can see in all panels of the figure that the slope of the second order is closer to the numerical one.

In Fig. 5, the same sets of variables are plotted as a function of x at two points in time. The time $t=1$ represents the point at which the source vanishes, meaning that all particles are injected, whereas $t=2$ represents a point in time where the particles have diffused for some time without an additional source. In this spatial distribution, we see again that the nonlinear solution has a broader shape than the linear solution (again represented by the zeroth order approximation). The numerical solution and the analytical approximation of the nonlinear solution lie above the linear one in the tails and beneath it in the center, corresponding to a higher effective diffusion coefficient. The quality of the analytical approximation increases with the order of the approximation. Except for singular points or small intervals, the second order approximation always gives a better fit than the first order in this figure.

IV. GREEN'S FUNCTION FOR A DIFFUSION EQUATION IN A SPHERICAL-SYMMETRIC SYSTEM

In Sec. III, we discussed the nonlinear diffusion problem in a Cartesian geometry. For a number of applications, however, a spherical geometry is needed. Limiting the consideration to pure nonlinear diffusion, i.e., neglecting both advection and adiabatic energy changes, the normalized diffusion equation reads as follows:

$$\frac{\partial f}{\partial t} = \frac{1}{r^2}\frac{\partial}{\partial r}\left(D(f)r^2\frac{\partial f}{\partial r}\right) + Q(r,t). \tag{23}$$

The diffusion coefficient $D(f)$ is given by $D(f) = D_0|\frac{\partial f}{\partial x}|^{\nu}$. A solution to the linear version of this equation (with $D_0 = 1$ and $\nu = 0$) has been found, e.g., by Webb and Gleeson (1977) for vanishing f in the limit $r \to \infty$. To be more precise, the solution to our problem derives from the calculations that Webb and Gleeson (1977) used to solve the equation

$$\frac{\partial F}{\partial t} = \frac{1}{G(x)}\frac{\partial}{\partial x}\left(E(x)\frac{\partial F}{\partial x}\right) + \delta(x-x_0)\delta(t-t_0), \tag{24}$$

for the boundaries $x=0$ and $x=\infty$ and $E(x) = G(x)$. There were only some minor adjustments necessary to make this setup fit our problem [for example taking $G(x) = x^2$]. The case for $D_0 \neq 1$ will be discussed below. The appropriate Green's formula for the specific problem reads

$$f(r,t) = \frac{1}{r^2}\int_0^t dt' \int_0^{\infty} dr' r'^2 Q(r',t')G(r',r,t-t'), \tag{25}$$

and the Green's function is given by

$$G(r',r,t-t') = \frac{r}{r'}\frac{1}{2\sqrt{\pi(t-t')}} \times \left(\exp\left(-\frac{(r'-r)^2}{4(t-t')}\right) - \exp\left(-\frac{(r'+r)^2}{4(t-t')}\right)\right). \tag{26}$$

If the source Q takes again the following form,

$$Q(r,t) = S_0(t-t^2)\delta(r-\hat{r}), \tag{27}$$

we obtain

$$f(r,t) = \int_0^t dt' \frac{\hat{r}}{r}(t'-t'^2)\frac{1}{2\sqrt{\pi(t-t')}} \times \left(\exp\left(-\frac{(\hat{r}-r)^2}{4(t-t')}\right) - \exp\left(-\frac{(\hat{r}+r)^2}{4(t-t')}\right)\right). \tag{28}$$

For Eq. (23), the same pertubative expansion in terms of the nonlinearity exponent ν as for the Cartesian case can be performed. Take $D_0 = 1$ for the equation and define the operator

$$\mathcal{L}_{\text{rad}} = \frac{\partial}{\partial t} - \frac{1}{r^2}\frac{\partial}{\partial r}\left(r^2\frac{\partial}{\partial r}\right), \tag{29}$$

and after the expansion of f in a very similar way as it has been done for Eqs. (11) and (12), and sorting the terms in orders of ν, the resulting expansion equations are as follows:

$$\mathcal{L}_{\text{rad}} f_0 = Q_0(r,t), \tag{30}$$

$$\mathcal{L}_{\text{rad}} f_1 = -(1+\ln(|f_{0,r}|))f_{0,rr} - \frac{1}{r}\ln(|f_{0,r}|)f_{0,r} = Q_1(r,t), \tag{31}$$

$$\begin{aligned}\mathcal{L}_{\text{rad}} f_2 = &-\frac{2}{r}\ln(|f_{0,r}|)f_{1,r} - \frac{2}{r}f_{1,r} \\ &-\ln(|f_{0,r}|)f_{1,rr} - \frac{1}{f_{0,r}}f_{1,r}f_{0,rr} - f_{1,rr} + \ln(|f_{0,r}|)f_{0,rr} \\ &+\frac{\ln^2(|f_{0,r}|)}{2}f_{0,rr} + \ln^2|f_{0,r}|\frac{f_{0,r}}{r} = Q_2(r,t).\end{aligned} \tag{32}$$

All these equations can be solved with Green's function, the required derivatives can be derived as well. The complete set of solutions reads as follows:

$$f^n(r,t) = \int_0^{\infty} dr' \int_0^t dt' \frac{rr'^2}{r^2} Q_n(r',t')G(r',r,t-t'), \tag{33}$$

$$f_r^n(r,t) = \int_0^{\infty} dr' \int_0^t dt' \frac{-2r'^2}{r^3} Q_n(r',t')G(r',r,t-t') + \int_0^{\infty} dr' \int_0^t dt' \frac{r'^2}{r^2} Q_n(r',t')G_r(r',r,t-t'), \tag{34}$$

$$\begin{aligned}f_{rr}^n(r,t) = &\int_0^{\infty} dr' \int_0^t dt' \frac{6r'^2}{r^4} Q_n(r',t')G(r',r,t-t') \\ &+\int_0^{\infty} dr' \int_0^t dt' \frac{-4r'^2}{r^3} Q_n(r',t')G_r(r',r,t-t') \\ &+\int_0^{\infty} dr' \int_0^t dt' \frac{r'^2}{r^2} Q_n(r',t')G_{rr}(r',r,t-t').\end{aligned} \tag{35}$$

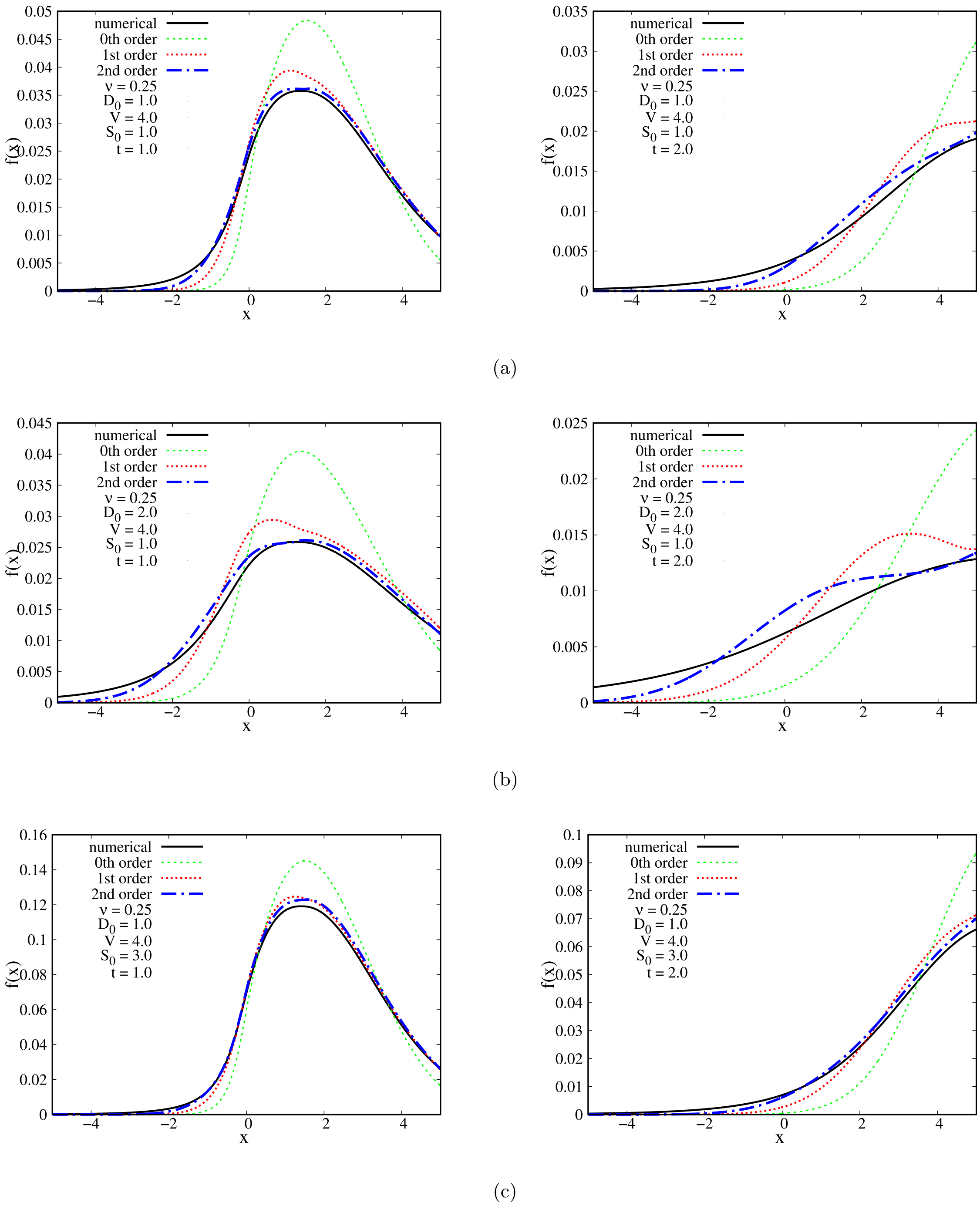

FIG. 5. Solution for a pulse-like particle source and variations of the parameters S_0, D_0, and V with a fixed nonlinearity parameter $\nu = \frac{1}{4}$: (a) $S_0 = 1$, $D_0 = 1$, $V = 4$, (b) $S_0 = 1$, $D_0 = 2$, $V = 4$, and (c) $S_0 = 3$, $D_0 = 1$, $V = 4$, and at times $t = 1$ (left) and $t = 2$ (right) from the source.

In Fig. 6, an example for a number of numerical solutions and the analytical approximation up to the second order in ν is given. The plots represent solutions of Eq. (23) with a source $Q = \delta(r-3)(t-t^2)$. The plot shows the analytical approximations and the numerical results for different ν and at one of three different points in space r. The first is exactly at the source at $r = 3$, the second $r = 2$, i.e., nearer to the origin of the chosen system of coordinates than the source, and the third point at $r = 4$ is chosen to have a greater distance from the origin than

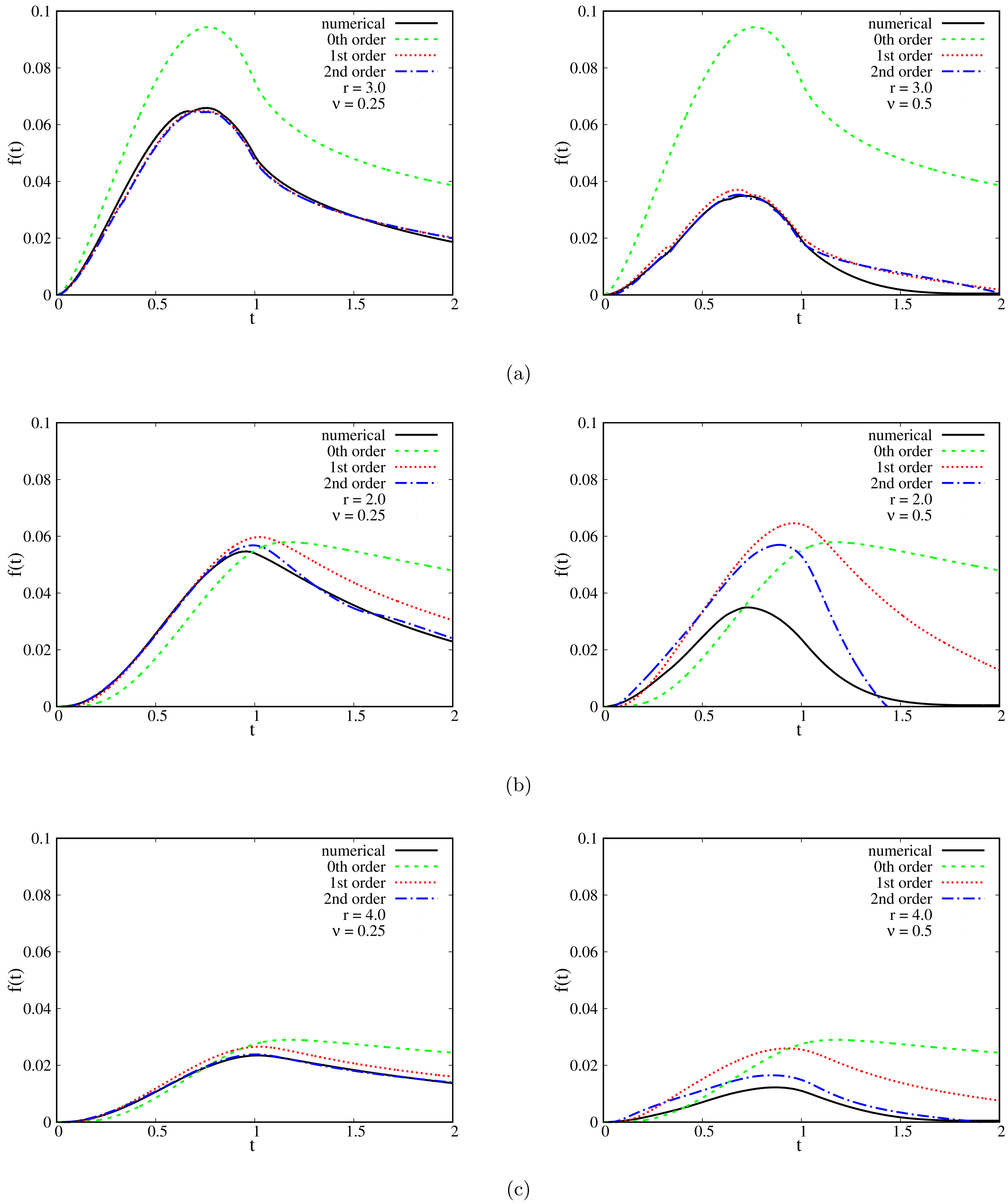

FIG. 6. Solution of Eq. (23) up to the second order, for a pulse like source. The parameters are $\nu = \frac{1}{4}$ (left) and $\nu = \frac{1}{2}$ (right) at the radial distances of $r = 3$ (a), $r = 2$(b), and $r = 4$ (c).

the source. As expected, the first-order approximation is acceptable to describe the numerical solutions for low ν or near the source, and it works less well for higher ν and further away from the source, while the second-order approximation does generally speaking a better job of describing the numerical solution. One can see two exceptions of this statement in the upper right and the middle right panel of Fig. 6. The first one shows the solutions at the source with a fairly high nonlinearity parameter $\nu = 0.5$, where the second order approximation does not seem to differ much from the first order approximation. The second panel has $r = 2$ and $\nu = 0.5$. In this panel, the second order approximation does not show great precision in describing the numerical solution. This may be due to the used numerical scheme that was used for solving the integrals. As in the Cartesian case, the solution does not reach the level expected from a linear diffusion equation, represented here by the zeroth order approximation, due to faster diffusing particles, and appears to decrease much quicker.

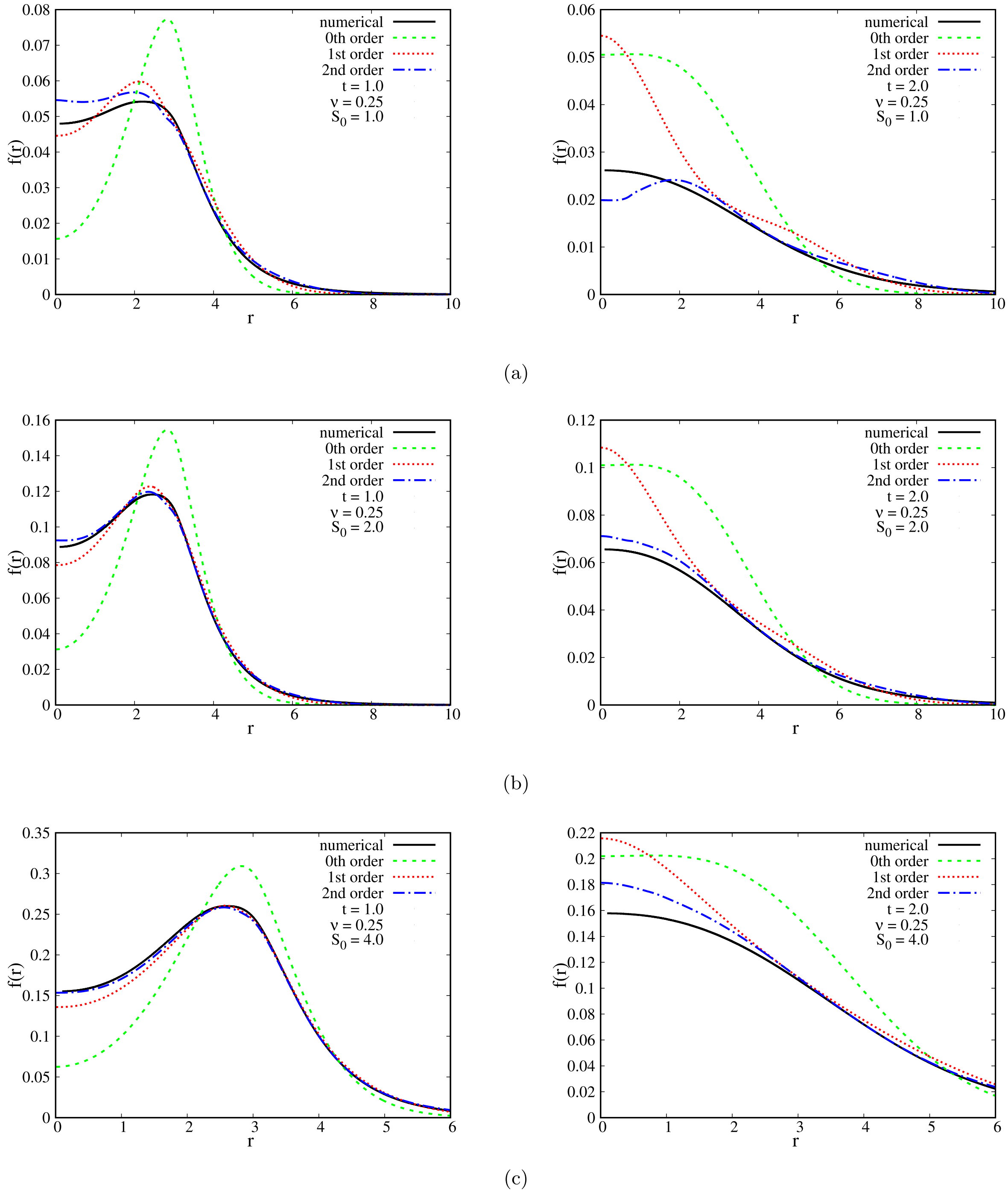

FIG. 7. Solution of Eq. (23) up to the second order, for a pulse like source. The nonlinearity parameter was chosen to be $\nu = \frac{1}{4}$ with the source strength S chosen as: (a) $S_0 = 1$, (b) $S_0 = 2$, and (c) $S_0 = 4$. The plotting times are $t = 1$ (left) and $t = 2$ (right).

As mentioned before, the Green's funtion we took from Webb and Gleeson (1977) is based on the assumption that $E(x) = G(x)$. However, this is not the case for $D_0 \neq 1$, so that it seems that our method is only applicable to this special case of $D_0 = 1$, but because we have no convection term in Eq. (23) we can make a simple calculation to get solutions for any arbitrary constant value of D_0. Say $D = D_0|f_r(r,t)|^{-\nu}$ with $D_0 \neq 1$ and define the function $g(r,t) = f(r, \frac{t}{D_0})$. It follows

$$\begin{aligned} g_t(r,t) &= \frac{1}{D_0} f_{\frac{t}{D_0}}\left(r, \frac{t}{D_0}\right) \\ &= \frac{1}{D_0 r^2}\frac{\partial}{\partial r}\left(r^2 D_0 \left|f_r\left(r,\frac{t}{D_0}\right)\right|^{-\nu} f_r\left(r,\frac{t}{D_0}\right)\right) + \frac{Q_0}{D_0} \\ &= \frac{1}{r^2}\frac{\partial}{\partial r}\left(r^2 |g_r(r,t)|^{-\nu} g_r(r,t)\right) + \frac{Q_0}{D_0}. \end{aligned} \tag{36}$$

So the function g satisfies the same differential equation with $D_0 \rightarrow 1$ and $Q_0 \rightarrow \frac{Q_0}{D_0}$. We are able to find a solution for this equation as seen above and only have to look at $g(r, D_0 \cdot t) = f(r,t)$ to find the solution for $f(r,t)$. Considering this, we only have to look at the differences in our solution that occur with changes of S_0. Figure 7 shows the spatial distribution for three different values of S_0 at two different points in time $t = 1$ and $t = 2$. The first two panels of Fig. 7 are the spatial version of the left column of Fig. 6, showing that the approximation tends to be more precise when we look at larger values of r. Yet again the second order approximation does perform better in comparison to the first order.

V. SUMMARY AND CONCLUSIONS

With the present work, we have continued our study of nonlinear diffusion of energetic particles. Since this topic has received considerable attention in recent years, analytical and semi-analytical results can serve as valuable guides for further more comprehensive modeling efforts. Consequently, we have expanded our previous work (Litvinenko *et al.*, 2017; Litvinenko *et al.*, 2019) in two ways.

First, instead of employing an integral method as in the case of pure nonlinear diffusion, we have applied an expansion technique to the advection-diffusion equation and obtained linear equations that are semi-analytically solvable with fundamental solutions. As we have demonstrated, this allows a simple systematic analysis of the effect of nonlinear diffusion for the cases of constant and spatially varying advection, which can incorporate time-varying source functions. Within the framework of our formulation of the nonlinear diffusion coefficient being proportional to $|\nabla f|^{-\nu}$, we found that the approximation is already very useful for the first order in the nonlinearity parameter ν provided that $\nu < 0.5$. This first-order and second-order approximation is most sensitive to the strength of the nonlinear diffusion and has visible change when altering the velocity. Furthermore, the approximation does increase with rising source strength when keeping the other parameters constant.

Second, we have extended the formalism from one-dimensional, Cartesian to radially symmetric geometry. The latter can, to a good approximation, be attributed to various astrophysical systems and allows us to treat the nonlinear diffusion problems on larger scales away from the source. The findings are qualitatively similar to the Cartesian case: the first-order approximation is acceptable to describe the numerical solutions for low ν or near the source, and the nonlinear diffusion is more effective than the linear one to transport particles away from the source, leading to intensity levels being generally lower than those of the linear case.

The expansion technique has some clear advantages in comparison to our previous models. In Litvinenko *et al.* (2017), we were able to give analytical approximations for a nonlinear diffusion advection equation, but only in the presence of a constant source. In Litvinenko *et al.* (2019), we were able to give approximations for nonlinear diffusion and a time-dependent source, but we made the assumption of symmetry of the particle distribution, which is not compatible with an additional advection. Now we were able to combine advection, time dependent sources, and analytical approximations, this way significantly expanding the applicability. Furthermore, we were able to extend our calculations to nonlinear diffusion in a spherical geometry, which could also not be achieved by the methods used in Litvinenko *et al.* (2019) because again the symmetry assumption is violated when a source is placed at $r \neq 0$. We were also able to show that the quality of the approximation most of the times does increase with the use of a higher order. From Eq. (5) alone, one could not tell that the $n+1$th approximation has a better quality of representing the complete solution than the nth approximation. But after looking at all the varieties of setups and systems we analyzed in this paper, we can feel safe enough to say,\ that in fact an increase in the used order of approximation does increase the quality of the approximation. The approximate solutions derived here extend the toolbox of easy-to-use solutions to nonlinear diffusion equations and will be used in future work to efficiently test whether these equations are better suited to describe energetic particles in astrophysical systems, particularly in the heliosphere, for which the most detailed and, thus, insightful observations are available. More generally, the new solutions illustrate the accuracy and utility of the pertubative approach by Bender *et al.* (1991) in nonlinear transport problems. To emphasize the wide applicability of the method described in this paper, similar calculations have been done for different partial differential equations which are discussed in the Appendix.

APPENDIX: TWO ADDITIONAL ILLUSTRATIVE EXAMPLES

To demonstrate that the method presented in this paper has a wide range of possible applications, we now apply it to two different nonlinear transport equations.

1. Effect of a diffusion coefficient with an intrinsic finite maximum

The equation used in the main text has the feature that the diffusion coefficient grows to infinity with a vanishing gradient, so the numerical code had to employ an upper limit for this coefficient to run properly. One can of course implement a different diffusion coefficient D_{eff} that has the same values in the limits of $\nu \rightarrow 0$ and $f_x \rightarrow 0$. Take a look at the following equation with λ_0 and D_1 being constants:

$$\frac{\partial f}{\partial t} + V\frac{\partial f}{\partial x} = \frac{\partial}{\partial x}\left(\frac{D_1}{\left|\frac{\partial f}{\partial x}\right|^{\nu} + \lambda_0}\frac{\partial f}{\partial x}\right) + S. \tag{A1}$$

For $|\frac{\partial f}{\partial x}|^{\nu} \gg \lambda_0$, this equation reads as the one in the main part of the paper, but the effective diffusion coefficient remains finite for

$\frac{\partial f}{\partial x} = 0$. For a comparison between this model and our main equation, one has to relate the parameters of the two equations. Define the parameters of the equations used in the main text by D_0 as the diffusion coefficient and $D_{\max}$ as the upper limit of the effective diffusion coefficient and take the limit of $\nu = 0$ and $f_x = 0$. This results in the two equations

$$D_0 = \frac{D_1}{1+\lambda_0}, \tag{A2}$$

$$D_{\max} = \frac{D_1}{\lambda_0}. \tag{A3}$$

With these equations, one can link one model to the other to get comparable results. If we expand f in Eqs. (A1) as in (5), we can proceed in a similar manner as before.

The transport equation can be read as

$$f_t + Vf_x = D_1\left(1 - \nu\frac{|f_x|^\nu}{|f_x|^\nu + \lambda_0}\right)\frac{f_{xx}}{|f_x|^\nu + \lambda_0} + S(x,t). \tag{A4}$$

We now have to evaluate the occurring terms of this equation in the same manner as we have done in the main part of the paper. This results in a set of equations for the following expressions:

$$\begin{aligned}\ln|f_x| &\approx \ln|f_{0,x}| + \nu\frac{f_{1,x}}{f_{0,x}} + \nu^2\cdots\\ |f_x|^\nu &\approx 1 + \nu\ln|f_x| + \frac{\nu^2}{2}\ln^2|f_x| \approx 1 + \nu\ln|f_{0,x}|\\ g(\nu) &\approx \frac{1}{|f_x|^\nu + \lambda_0} \approx g(0) + \nu\dot{g}(0) + \frac{1}{2}\nu^2\ddot{g}(0) + \cdots.\end{aligned} \tag{A5}$$

To determine the approximation of the function g, we need to look at the required derivatives.

$$\begin{aligned}g(\nu) &= \frac{1}{1 + \nu\ln|f_x| + \nu^2\cdots + \lambda_0}\\ \dot{g}(\nu) &= -\frac{\ln|f_x| + \nu(\ln|f_x|)' + \nu\ln^2|f_x| + \nu^2\cdots}{(1 + \nu\ln|f_x| + \nu^2\cdots + \lambda_0)^2}\\ \ddot{g}(\nu) &= \frac{2\left(\ln|f_x| + \nu(\ln|f_x|)' + \nu\ln^2|f_x| + \nu^2\cdots\right)^2}{(1 + \nu\ln|f_x| + \nu^2\cdots + \lambda_0)^3}\\ &\quad - \frac{\left(2(\ln|f_x|)' + \ln^2|f_x| + \nu\cdots\right)}{(1 + \nu\ln|f_x| + \nu^2\cdots + \lambda_0)^2}\\ g(0) &= \frac{1}{1+\lambda_0}\\ \dot{g}(0) &= -\frac{1}{(1+\lambda_0)^2}\ln|f_{0,x}|\\ \ddot{g}(0) &= \frac{2}{(1+\lambda_0)^3}\ln^2|f_{0,x}| - \frac{2}{(1+\lambda_0)^2}\frac{f_{1,x}}{f_{0,x}} - \frac{\ln^2|f_{0,x}|}{(1+\lambda_0)^2}.\end{aligned} \tag{A6}$$

All those expressions can now be inserted into the transport equation, and we get the following equations up to the second order:

$$\mathcal{L}_c = \frac{\partial}{\partial t} + V\frac{\partial}{\partial x} - \frac{D_1}{1+\lambda_0}\frac{\partial^2}{\partial x^2}, \tag{A7}$$

$$\mathcal{L}_c f_0 = S, \tag{A8}$$

$$\mathcal{L}_c f_1 = -D_1\frac{1 + \ln|f_{0,x}|}{(1+\lambda_0)^2}f_{0,xx}, \tag{A9}$$

$$\begin{aligned}\mathcal{L}_c f_2 &= -D_1\frac{\ln|f_{0,x}| + 1}{(1+\lambda_0)^2}f_{1,xx} + D_1\frac{\ln^2|f_{0,x}| + 2\ln|f_{0,x}|}{(1+\lambda_0)^3}f_{0,xx}\\ &\quad - D_1\frac{\frac{1}{2}\ln^2|f_{0,x}| + \ln|f_{0,x}|}{(1+\lambda_0)^2}f_{0,xx} - D_1\frac{f_{1,x}}{(1+\lambda_0)^2 f_{0,x}}f_{0,xx}.\end{aligned} \tag{A10}$$

In Fig. 8, one can see the result up to the second order in ν for a setup with a source $S = S_0(t - t^2)\delta(x)$ and the combinations $x \in \{0, 1\}$ and $\nu \in \{\frac{1}{4}, \frac{1}{2}\}$. The parameters D_1 and λ_0 have been chosen, so that the limits $\nu = 0$ and $f_x = 0$ represent the same values as resulting from Eq. (4) with the constant speed $V = 4$ and $D_0 = 1$ and the upper limit $D_{\max} = 10^3$. Comparison of the upper right panel of Fig. 8 with the upper left panel of Fig. 4 shows that the results are very similar, pointing out that for the value of $D_{\max} = 10^3$ both equations do in fact represent the same physical model.

It can also be seen that the approximation up to the second order in ν departs from the numerical for $\nu = \frac{1}{2}$. In the lower right panel of Fig. 8, it additionally develops a second bounce that is not plausible from a physics point of view. So for a strong nonlinear case, $\nu \geq \frac{1}{2}$, it is necessary to include approximations of higher order.

2. Effect of a diffusion coefficient being proportional to a power of the distribution *f*

Another example that can be treated very well with our approach was proposed by Kath and Cohen (1982) in the form of a nonlinear diffusion equation reading as follows:

$$\frac{\partial f}{\partial t} = \frac{\partial}{\partial x}\left(D_0\cdot f^\nu\frac{\partial f}{\partial x}\right). \tag{A11}$$

According to Kath and Cohen (1982), this equation has physical application in several different areas, for example, in the study of porous media, or radiative heat transfer by Marshak waves. For Eq. (A11), one can find a similiarity solution of the form

$$f(x,t) = t^{\frac{-1}{2+\nu}}g(\xi), \tag{A12}$$

where $\xi = \frac{x}{t^{\frac{1}{2+\nu}}}$ and g is given by the differential equation

$$\frac{-1}{2+\nu}(g + \xi\dot{g}) = \nu g^{\nu-1}\dot{g}^2 + g^\nu\ddot{g}. \tag{A13}$$

This differential equation can be solved analytically and has the solution

$$g(\xi) = \left[C - \frac{1}{2}\frac{\nu}{2+\nu}\xi^2\right]^{\frac{1}{\nu}}. \tag{A14}$$

C is a constant that can be determined by the total number of particles injected. For further calculations, define the operator $\mathcal{L}_K$ that will be our central operator after the expansion,

$$\mathcal{L}_K = \frac{\partial}{\partial t} + V\frac{\partial}{\partial x} - D_0\frac{\partial^2}{\partial x^2}. \tag{A15}$$

Adding constant advection and a source S, A11 reads as

$$\begin{aligned}\frac{\partial f}{\partial t} + V\frac{\partial f}{\partial x} &= D_0\frac{\partial}{\partial x}\left(f^\nu\frac{\partial f}{\partial x}\right) + S\\ &= D_0\nu f^{\nu-1}f_x^2 + D_0 f^\nu f_{xx} + S.\end{aligned} \tag{A16}$$

First we take a look at the following terms:

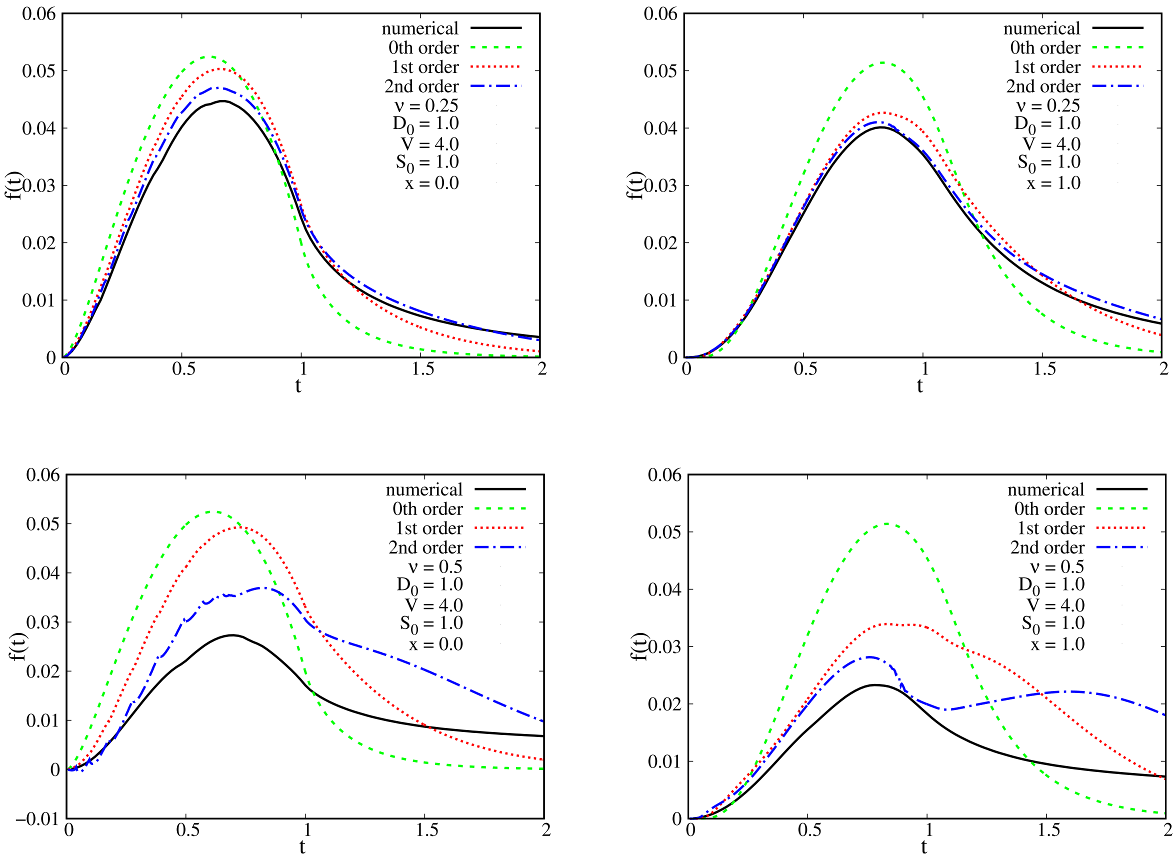

FIG. 8. Solution of Eq. (A1) up to the second order, for a pulse like source. The parameters are $D_0 = 1$ and $D_{\max} = 10^3$ with $V = 4$ for $x = 0$ and $\nu = \frac{1}{4}$(upper left), $x = 1$ and $\nu = \frac{1}{4}$(upper right), $x = 0$ and $\nu = \frac{1}{2}$(lower left) and $x = 1$ and $\nu = \frac{1}{2}$(lower right).

$$
\begin{aligned}
f^{\nu} &= \exp\left(\nu \ln(f)\right) \approx 1 + \nu \ln(f) + \frac{1}{2}\nu^2 \ln^2(f) \\
f^{\nu-1} &= \frac{f^{\nu}}{f} \approx \frac{1 + \nu \ln(f) + \cdots}{f}.
\end{aligned} \tag{A17}
$$

Now we can examine a useful form for all parts of the equation above,

$$
\begin{aligned}
h(\nu) &= \ln(f) = \ln\left(f_0 + \nu f_1 + \nu^2 f_2 + \cdots\right) \\
g(\nu) &= \frac{1}{f} = \frac{1}{f_0 + \nu f_1 + \nu^2 f_2 + \cdots} \\
l(\nu) &= \frac{\ln(f)}{f} = \frac{\ln\left(f_0 + \nu f_1 + \nu^2 f_2 + \cdots\right)}{f_0 + \nu f_1 + \nu^2 f_2 + \cdots}.
\end{aligned} \tag{A18}
$$

To develop the equation up to the second order in ν, the functions above have to be Taylor-developed as follows:

$h(\nu)$ has to be developed up to the first order, $g(\nu)$ up to the first order, and $l(\nu)$ up to the zeroth order

$$
\begin{aligned}
h(\nu) &\approx \ln(f_0) + \nu \frac{f_1}{f_0} \\
g(\nu) &\approx \frac{1}{f_0} - \nu \frac{f_1}{f_0^2} \\
l(\nu) &\approx \frac{\ln(f_0)}{f_0}.
\end{aligned} \tag{A19}
$$

After inserting this result into the previous equations and sorting with respect to the order of ν, we get a complete set of equations,

$$
\mathcal{L}_K f_0 = S, \tag{A20}
$$

$$
\mathcal{L}_K f_1 = D_0 \left(\frac{f_{0,x}^2}{f_0} + \ln|f_0| f_{0,xx} \right), \tag{A21}
$$

$$
\begin{aligned}
\mathcal{L}_K f_2 = D_0 \Bigg(& \frac{2 f_{0,x}}{f_0} f_{1,x} - \frac{f_1 f_{0,x}^2}{f_0^2} + \frac{\ln|f_0| f_{0,x}^2}{f_0} + \ln|f_0| f_{1,xx} \\
& + \frac{f_1}{f_0} f_{0,xx} + \frac{1}{2} \ln^2|f_0| f_{0,xx} \Bigg).
\end{aligned} \tag{A22}
$$

In Fig. 9, the results up to second order of ν with the parameters of $D_0 = 1$, $\nu = \frac{1}{4}$ at $x = 0$ are presented. The source was chosen as before to be pulse like of the form $S = S_0(t - t^2)\delta(x)$. The results represent a quite accurate approximation of the distribution function for low ν although there is an area just behind the switch-off-point of the source in time, where the approximation has negative values, which is by no means physical, but this effect is expected to vanish by using higher orders of approximation.

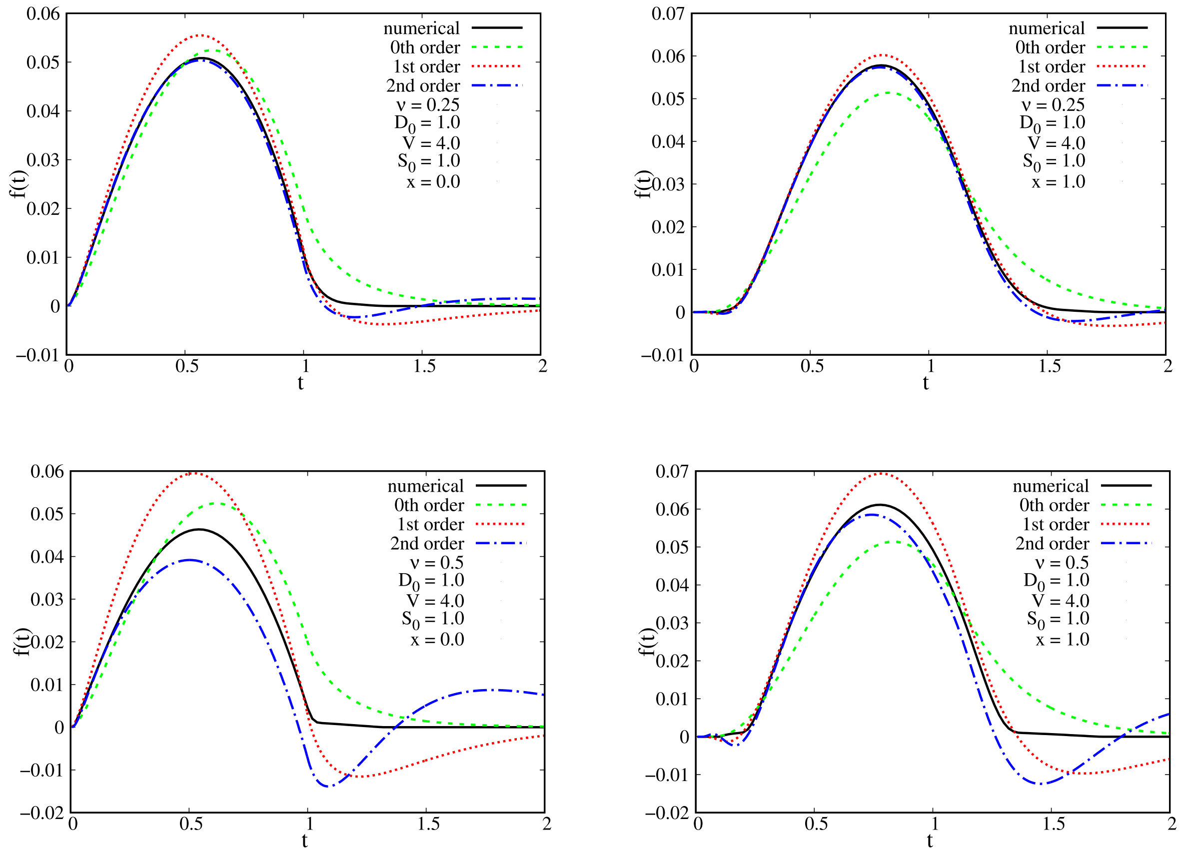

FIG. 9. Solution of Eq. (A11) up to the second order, for a pulse like source. The parameters are $D_0 = 1, V = 4$ for $\nu = \frac{1}{4}$ at $x = 0$ and $x = 1$ (upper row) and $\nu = \frac{1}{2}$ at $x = 0$ and $x = 1$.

DATA AVAILABILITY

Data sharing is not applicable to this article as no new data were created or analyzed in this study.

REFERENCES

Amato, E. and Blasi, P., "Cosmic ray transport in the galaxy: A review," Adv. Space Res. **62**, 2731–2749 (2018).

Bender, C. M., Boettcher, S., and Milton, K. A., "A new perturbative approach to nonlinear partial differential equations," J. Math. Phys. **32**, 3031–3038 (1991).

Bender, C. M., Milton, K. A., Pinsky, S. S., and Simmons, L. M., "A new perturbative approach to nonlinear problems," J. Math. Phys. **30**, 1447–1455 (1989).

Bykov, A. M., Ellison, D. C., Osipov, S. M., and Vladimirov, A. E., "Magnetic field amplification in nonlinear diffusive shock acceleration including resonant and non-resonant cosmic-ray driven instabilities," Astrophys. J. **789**, 137 (2014).

Diesing, R. and Caprioli, D., "Spectrum of electrons accelerated in supernova remnants," Phys. Rev. Lett. **123**, 071101 (2019).

dos Santos, M. A. F., "Analytic approaches of the anomalous diffusion: A review," Chaos Solitons Fractals **124**, 86–96 (2019).

Dresner, L., *Similarity Solutions of Nonlinear Partial Differential Equations*, Research Notes in Mathematics (Pitman Advanced Publications Program, 1983).

Fahr, H.-J. and Fichtner, H., "The influence of pick-up ion-induced wave pressures on the dynamics of the mass-loaded solar wind," Sol. Phys. **137**, 355–363 (1992).

Hartmann, C. and Weimar, M., "Besov regularity of solutions to the p-poisson equation in the vicinity of a vertex of a polygonal domain," Results Math. **73**, 41 (2018).

Holcomb, C. and Spitkovsky, A., "On the growth and saturation of the gyroresonant streaming instabilities," Astrophys. J. **882**, 3 (2019).

Isenberg, P. A., "Interaction of the solar wind with interstellar neutral hydrogen: Three-fluid model," J. Geophys. Res. **91**, 9965–9972, https://doi.org/10.1029/JA091iA09p09965 (1986).

Kath, W. L. and Cohen, D. S., "Waiting-time behavior in a nonlinear diffusion equation," Stud. Appl. Math. **67**, 79–105 (1982).

Lee, M. A., Mewaldt, R. A., and Giacalone, J., "Shock acceleration of ions in the heliosphere," Space Sci. Rev. **173**, 247–281 (2012).

Litvinenko, Y. E., Fichtner, H., and Walter, D., "Anomalous transport of cosmic rays in a nonlinear diffusion model," Astrophys. J. **841**, 57 (2017).

Litvinenko, Y. E., Walter, D., and Fichtner, H., "A nonlinear energetic particle diffusion model with a variable source," AIP Adv. **9**, 055005 (2019).

Moloto, K. D., Engelbrecht, N. E., and Burger, R. A., "A simplified *ab initio* cosmic-ray modulation model with simulated time dependence and predictive capability," Astrophys. J. **859**, 107 (2018).

Nava, L., Gabici, S., Marcowith, A., Morlino, G., and Ptuskin, V. S., "Non-linear diffusion of cosmic rays escaping from supernova remnants—I. The effect of neutrals," Mon. Not. R. Astron. Soc. **461**, 3552–3562 (2016).

Nava, L., Recchia, S., Gabici, S., Marcowith, A., Brahimi, L., and Ptuskin, V., "Non-linear diffusion of cosmic rays escaping from supernova remnants—II. Hot ionized media," Mon. Not. R. Astron. Soc. **484**, 2684–2691 (2019).

Perri, S., Amato, E., and Zimbardo, G., "Transport of relativistic electrons at shocks in shell-type supernova remnants: Diffusive and superdiffusive regimes," Astron. Astrophys. **596**, A34 (2016).
Philip, J. R., "n-diffusion," Aust. J. Phys. **14**(1), 1 (1961).
Ptuskin, V., Zirakashvili, V., and Seo, E.-S., "Spectra of cosmic-ray protons and helium produced in supernova remnants," Astrophys. J. **763**, 47 (2013).
Ptuskin, V. S. and Zirakashvili, V. N., "Limits on diffusive shock acceleration in supernova remnants in the presence of cosmic-ray streaming instability and wave dissipation," Astron. Astrophys. **403**, 1–10 (2003).
Ptuskin, V. S., Zirakashvili, V. N., and Plesser, A. A., "Non-linear diffusion of cosmic rays," Adv. Space Res. **42**, 486–490 (2008).
Shalchi, A., "Analytical description of the time-dependent perpendicular transport of energetic particles," Astrophys. J. **864**, 155 (2018).
Vázquez, J. L., "The mathematical theories of diffusion: Nonlinear and fractional diffusion," in *Nonlocal and Nonlinear Diffusions and Interactions: New Methods and Directions: Cetraro, Italy 2016*, edited by M. Bonforte and G. Grillo (Springer International Publishing, Cham, 2017), pp. 205–278.
Webb, G. M. and Gleeson, L. J., "Green's theorem and Green's functions for the steady-state cosmic-ray equation of transport," Astrophys. Space Sci. **50**, 205–223 (1977).
Wiener, J., Zweibel, E. G., and Ruszkowski, M., "Cosmic ray acceleration of cool clouds in the circumgalactic medium," Mon. Not. R. Astron. Soc. **489**, 205–223 (2019).
Yosida, K., *Functional Analysis, Grundlehren Der Mathematischen Wissenschaften* (Springer-Verlag, 1980).
Zirakashvili, V. N., "Induced scattering and two-photon absorption of Alfvén waves with arbitrary propagation angles," J. Exp. Theor. Phys. **90**, 810–816 (2000).